Segmentation of rifts through structural inheritance: Creation of the Davis Strait

P. J. Heron[1], A. L. Peace[2], K. McCaffrey[1], J. K. Welford[2], R. Wilson[3], and R. N. Pysklywec[4]

[1]Durham University, Department of Earth Sciences, Durham, United Kingdom.
[2]Memorial University of Newfoundland, Department of Earth Sciences, St. John's, Newfoundland, Canada.
[3]BP Exploration, Sunbury-on-Thames, Middlesex, UK.
[4]University of Toronto, Department of Earth Sciences, Toronto, Ontario, Canada.

Key Points:

- The role of mantle sutures during Mesozoic rifting and Cenozoic ocean basin development in Laurentia has not been studied
- We present 3-D models that reproduce first order tectonics of Labrador Sea, Davis Strait, Baffin Bay through mantle suture reactivation
- The obliquity of the mantle suture to the extension preserves continental lithosphere, interpreted as the creation of the Davis Strait

Corresponding author: Philip J. Heron, philip.j.heron@durham.ac.uk

Abstract

Mesozoic-Cenozoic rifting between Greenland and North America created the Labrador Sea and Baffin Bay, while leaving preserved continental lithosphere in the Davis Strait which lies between them. Inherited crustal structures from a Palaeoproterozoic collision have been hypothesized to account for the tectonic features of this rift system. However, the role of mantle lithosphere heterogeneities in continental suturing has not been fully explored. Our study uses 3-D numerical models to analyze the role of crustal and sub-crustal heterogeneities in controlling deformation. We implement continental extension in the presence of mantle lithosphere suture zones and deformed crustal structures and present a suite of models analyzing the role of local inheritance related to the region. In particular, we investigate the respective roles of crust and mantle lithospheric scarring during an evolving stress regime in keeping with plate tectonic reconstructions of the Davis Strait. Numerical simulations, for the first time, can reproduce first order features that resemble the Labrador Sea, Davis Strait, Baffin Bay continental margins and ocean basins. The positioning of a mantle lithosphere suture, hypothesized to exist from ancient orogenic activity, produces a more appropriate tectonic evolution of the region than the previously proposed crustal inheritance. Indeed, the obliquity of the continental mantle suture with respect to extension direction is shown here to be important in the preservation of the Davis Strait. Mantle lithosphere heterogeneities are often overlooked as a control of crustal-scale deformation. Here, we highlight the sub-crust as an avenue of exploration in the understanding of rift system evolution.

1 Introduction

Numerous previous studies have shown the potential for mantle lithosphere structures to control the evolution of shallow tectonics [*Pysklywec and Beaumont*, 2004; *Heron et al.*, 2016; *Jourdon et al.*, 2017; *Phillips et al.*, 2018; *Salazar-Mora et al.*, 2018; *Balázs et al.*, 2018; *Schiffer et al.*, 2018; *Heron et al.*, 2019], highlighting a deep genesis for lithosphere-scale deformation [e.g., *Vauchez et al.*, 1997; *Holdsworth et al.*, 2001]. Reactivation of features formed through previous collisional or rifting events [*Wilson*, 1966] is well established and thought to occur along well-defined, pre-existing structures such as faults, shear zones or lithological contacts [*Holdsworth et al.*, 1997]. Such tectonic features exist in the present-day mantle lithosphere [*Morgan et al.*, 1994; *Lie and Husebye*, 1994; *Calvert et al.*, 1995; *Calvert and Ludden*, 1999; *Schiffer et al.*, 2014, 2016; *Hopper and Fischer*, 2015; *Biryol et al.*, 2016] and may relate to a deep mechanical weakness in the tectonic plate [*Pollack*, 1986; *Dunbar and Sawyer*, 1988, 1989; *Thomas*, 2006; *Bercovici and Ricard*, 2014; *Erdős et al.*, 2014; *Manatschal et al.*, 2015]. Here, through numerical modelling, we apply the basic tenets of inheritance and reactivation (e.g., the Wilson cycle) to the continental mantle lithosphere of West Greenland to understand the rift evolution of the Davis Strait (Figure 1).

The Labrador Sea, Davis Strait and Baffin Bay (Fig. 1a) formed due to Mesozoic to Cenozoic divergent motion between Greenland and North America [*Chalmers and Pulvertaft*, 2001; *Wilson et al.*, 2006; *Hosseinpour et al.*, 2013; *Peace et al.*, 2017; *Abdelmalak et al.*, 2018; *Peace et al.*, 2018a,b]. Rifting prior to the opening of the Labrador Sea may have started as early as the Late Triassic to Jurassic, based on ages obtained from dyke swarms in southwest Greenland that are interpreted to be related to early rifting [*Larsen et al.*, 2009]. Breakup from south to north between Greenland and Canada resulted in oceanic spreading in the Labrador Sea and eventually Baffin Bay [*Srivastava*, 1978; *Jackson et al.*, 1979; *Roest and Srivastava*, 1989; *Chian et al.*, 1995; *Welford and Hall*, 2013; *Welford et al.*, 2018]. These small ocean basins are connected through the Davis Strait in a 'dog-leg' shape (Fig. 1b), a bathymetric high comprising primarily of continental lithosphere where continental breakup did not fully occur [*Suckro et al.*, 2013], and the foci of the West Greenland Tertiary Volcanic Province [*Storey et al.*, 1998; *Peace et al.*, 2017; *Clarke and Beutel*, 2019].

Based on this history, a first order characterization of the West Greenland rift system (sometimes referred to as the NW Atlantic, e.g. *Abdelmalak et al.* [2018]) can be given in four points (later referred to as 'the checklist'):

1. Rifting south of Davis Strait in the Labrador Sea produced new oceanic crust;
2. Rifting north of Davis Strait in Baffin Bay produced new oceanic crust;
3. A right-stepping segmentation geometry (the Davis Strait) was formed to link Labrador Sea with Baffin Bay;
4. Continental crust is preserved in the Davis Strait during rifting.

The West Greenland-Eastern Canada realm comprises multiple Archean and Proterozoic geological domains, reflecting a complex, multi-phase evolution [e.g. *Kerr et al.*, 1997; *St-Onge et al.*, 2009; *Grocott and McCaffrey*, 2017]. The evolution of these domains, including their correlation to a pre-Cretaceous reconstruction is dealt with in detail in *van Gool et al.* [2002] and *St-Onge et al.* [2009], as such only the most salient points relevant to this study are reiterated here.

These Archean and Proterozoic domains, and the pre-existing structures they contain, likely influenced the Mesozoic-Cenozoic rifting, breakup and transform system development through the process of structural inheritance [*Watterson*, 1975; *Wilson et al.*, 2006; *Japsen et al.*, 2006; *Peace et al.*, 2017, 2018b,a]. This previous work has shown that crustal structural inheritance may have controlled the large-scale geometry of breakup and transform systems, the geometry and kinematics of rift-related faulting, and potentially also the location of rifting and breakup-related magmatism. As such it is important to understand the formation of the different basement units that comprise this study area (Fig. 1c). Principally, from north to south the study area herein comprises the following gross tectonic units: the Nagssugtoqidian and Torngat orogens; the North Atlantic Craton and the Nain Province; and the Makkovik Province and the Ketilidian Mobile Belt (Fig. 1).

The once continuous Archean North Atlantic Craton is now distributed between Greenland, northwest Scotland and Labrador (where it is called the Nain Province) [*St-Onge et al.*, 2009] (Fig. 1c-e). The North Atlantic Craton is bordered to the north and west by segments of Palaeoproterozoic orogenic belts that are tectonically related to the Trans-Hudson Orogen including the Nagssugtoqidian Orogen and Rinkian fold belt on the north side and the Torngat Orogen on the west side of the craton [*St-Onge et al.*, 2009].

To the north of the North Atlantic Craton lies the Nagssugtoqidian Orogen (Fig 1c). This is a belt of Palaeoproterozoic deformation and metamorphism in West Greenland considered to have developed simultaneously with the Torngat Orogen in northern Labrador [*van Gool et al.*, 2002]. Although the precise spatio-temporal relationship between these orogenic belts is questioned [*Scott*, 1999], they are interpreted to have formed part of the same Palaeoproterozoic passive margin prior to ocean closure and continental collision with the North Atlantic Craton and Nain Province [*van Gool et al.*, 2002; *Grocott and McCaffrey*, 2017].

The dynamics of West Greenland rifting and the preservation of the continental Davis Strait is currently a topic of active research, with lithospheric inheritance being discussed as a potential controlling mechanism [*Wilson et al.*, 2006; *Peace et al.*, 2017, 2018a,b]. In this study, we outline a two-phase tectonic history where mantle lithosphere inheritance is generated and then contributes to crustal deformation during subsequent rifting (Fig 2). We hypothesize a Palaeoproterozoic collision, that featured the North Atlantic Craton and produced the Nagssugtoqidian Orogen [*van Gool et al.*, 2002], would have left mantle lithosphere scarring during the continental suturing [e.g., *Calvert et al.*, 1995; *Vauchez et al.*, 1997; *Holdsworth et al.*, 2001]. Although there is no direct evidence of a mantle structure, deformation during the Nagssugtoqidian Orogen is thought to be on a lithospheric scale, rather than simply crustal scale [*Watterson*, 1975; *Grocott*, 1977;

van Gool et al., 2002], and as a result we consider that a mantle suture is likely to have been produced (Fig 2) [e.g., *Mickus and Keller*, 1992; *Morgan et al.*, 1994; *Lie and Husebye*, 1994; *Calvert et al.*, 1995; *Vauchez et al.*, 1997, 1998; *Steer et al.*, 1998; *Calvert and Ludden*, 1999; *Schiffer et al.*, 2014, 2016; *Hopper and Fischer*, 2015; *Biryol et al.*, 2016]. Indeed, *Watterson* [1975] first identified the Palaeoproterozoic Nagssugtoqidian orogenic belt as a lithosphere-scale boundary due to the presence of Cambrian age kimberlites that are cross-cut by Mesozoic pseudotachylytes, which was a finding later confirmed by *Grocott* [1977].

In this study, we model upper crust inheritance and a mantle lithosphere scar that approximates the shape and extent of the suture surrounding the North Atlantic Craton. Below, in a suite of numerical simulations, we analyse the influence of lithosphere inheritance for generating rift tectonics appropriate to the Labrador Sea, Davis Strait, and Baffin Bay.

2 Methods

The role of three-dimensional (3-D) lithosphere structure in a continental extension tectonic setting similar to that of the Davis Strait is investigated. The models are implemented in a high-resolution 3-D Cartesian box (Fig. 3), using the numerical code ASPECT [*Heister et al.*, 2017; *Kronbichler et al.*, 2012; *Bangerth et al.*, 2018a,b; *Rose et al.*, 2017], which uses the finite-element method to solve the system of equations that describes the motion of a highly viscous fluid. Specifically,we use a non-linear viscous flow (dislocation creep) and Drucker Prager plasticity for our model rheology [e.g., *Naliboff and Buiter*, 2015].

2.1 Experimental setup

The 3-D numerical experiments are conducted within a model domain of 800 km (x-axis) by 800 km (y-axis) and 600 km vertically (z-axis). The computational grid is uniform laterally, but resolution varies vertically with higher resolution prescribed in the top 80 km of the model (from the surface to 80 km depth). Below, the resolution becomes more coarse, with a reduction in resolution between 80 and 180 km, then finally the lowest resolution from 180 km depth to the bottom of the model (Supplementary Information Fig. S1). There are 1.7 million active cells in the model, with a horizontal resolution of ~1 km at the surface.

The 3-D simulations are very computationally expensive, producing 147 million degrees of freedom and needing around 80 Gb memory. For most cases, the models used 416 CPUs and took ~16,000 hours of computational time to generate 12 Myr of deformation on ComputeCanada's Niagara cluster [*Loken et al.*, 2010].

2.2 Governing equations

In this study, we solve the equations of conservation of momentum, mass and energy after assuming an incompressible medium with infinite Prandtl number:

$$-\nabla \cdot (2\mu\dot{\varepsilon}\mathbf{u}) + \nabla P = \rho\mathbf{g}, \tag{1}$$

$$\nabla \cdot \mathbf{u} = 0, \tag{2}$$

$$\rho C_P\left(\frac{\partial T}{\partial t} + \mathbf{u} \cdot \nabla T\right) - \nabla \cdot k\nabla T = pH. \tag{3}$$

In the equations above, μ is the viscosity, $\dot{\varepsilon}$ is the strain rate tensor, u is the velocity vector, k is the thermal conductivity, ρ is the density, C_p is the thermal heat capacity, H the internal heat production, P the pressure, g gravity, and T the temperature.

Different material parameters (in this case upper crust, lower crust, mantle lithosphere, asthenosphere, and scar) are represented by compositional fields that are advected with the flow. For each field (c_i), this formulation introduces an additional advection equation to the system of equations:

$$\frac{\partial c_i}{\partial x} + \mathbf{u} \cdot \nabla c_i = 0. \tag{4}$$

Equations 1-4 are solved using the finite element method, where the domain is discretized into quadrilateral/hexahedral finite elements and the solution (e.g., velocity, pressure, temperature and compositional fields) is expanded using Lagrange polynomials as interpolating basis functions (as outlined in *Glerum et al.* [2018]). In this study, we employ second order polynomials for velocity, temperature and composition and first order polynomials for pressure (Q2Q1 elements, *Donea and Huerta* [e.g., 2003]). The equations are solved using an iterative Stokes solver (for more details see *Kronbichler et al.* [2012]). The models are incompressible, but we apply the real density to the temperature equation.

We use a nonlinear viscous flow (dislocation creep) and Drucker-Prager plasticity for the model rheology and follow a setup similar to previous studies [e.g., *Huismans and Beaumont*, 2011; *Brune et al.*, 2014; *Naliboff and Buiter*, 2015; *Brune et al.*, 2017]. The viscosity for dislocation or diffusion creep is defined as:

$$\mu = 0.5A^{-\frac{1}{n}} \dot{\varepsilon_{ii}}^{\frac{(1-n)}{n}} \exp\left(\frac{E + PV}{nRT}\right) \tag{5}$$

where A is the viscosity prefactor, n is the stress exponent, $\dot{\varepsilon_{ii}}$ is the square root of the deviatoric strain rate tensor second invariant, E is activation energy, V is activation volume, and R is the gas exponent [*Karato and Wu*, 1993; *Karato*, 2008]. Here, we use the dislocation creep ($\mu_{(disl)}$; $n > 1$) equation form.

Viscosity is limited through one of two different 'yielding' mechanisms. Plasticity limits viscous stress through a Drucker Prager yield criterion, where the yield stress in 3-D is

$$\sigma_y = (6C\cos\varphi + 2P\sin\varphi)/(\sqrt{3}(3 + \sin\varphi)) \tag{6}$$

Above, C is cohesion and φ is the angle of internal friction. If φ is 0, the yield stress is fixed and equal to the cohesion (Von Mises yield criterion). When the viscous stress ($2\mu\varepsilon_{ii}$) exceeds the yield stress, the viscosity is rescaled back to the yield surface $\mu_y = \sigma_y/(2\dot{\varepsilon}_{ii})$, [e.g., *Thieulot*, 2011]. This method of plastic yielding is known as the Viscosity Rescaling Method (VRM) [*Willett*, 1992; *Kachanov*, 2004] and is implemented by locally rescaling the effective viscosity in such a way that the stress does not exceed the yield stress. In the models here, strain weakening is implemented for the internal friction angle and cohesion; they are linearly reduced by 50% of their value (from 20^o and 20 MPa [e.g., *Bos*, 2002]) as a function of the finite strain magnitude. This weakening occurs between 0 to 0.5 strain, which is a range used in the recent *Brune et al.* [2017] rifting study. Other strain ranges for weakening were tested and the findings are presented in Supplementary Information Figs. S2, S3, and S4.

Compositional fields (upper crust, lower crust, mantle lithosphere, asthenosphere, and scarring) can each be assigned individual values of thermal diffusivity, heat capacity, density, thermal expansivity, and rheological parameters (Table 1). If more than one compositional field is present at a given point (such as for a scar overlain on top of mantle lithosphere), viscosities are averaged with a harmonic scheme [e.g., *Glerum et al.*, 2018].

The rheological setup of these models closely follows that of *Naliboff and Buiter* [2015]. Table 1 outlines the rheological parameters used for the different compositional layers. The upper crust implements a wet quartzite flow law [*Rutter and Brodie*, 2004], lower crust applies wet anorthite [*Rybacki et al.*, 2006], and the mantle dry olivine [*Hirth and Kohlstedt*, 2003]. All the viscous pre-factors described in Table 1 are scaled to plane strain from uniaxial strain experiments.

An initial reference viscosity of 10^{22} Pa.s is applied to each compositional field in the models due to the strain rate dependence of viscosity and the lack of an initial guess for the strain rate for the first time-step [*Glerum et al.*, 2018]. This initial reference viscosity was changed in the setup of the numerical models, and not found to change the outcome of the study. During subsequent time-steps, the strain rate of the previous time-step is used as an initial guess for the iterative process. The final effective viscosity is capped by a (user-defined) minimum viscosity (set at 10^{18} Pa.s) and maximum viscosity (set at 10^{26} Pa.s) to avoid extreme excursions and to ensure stability of the numerical scheme. In the models presented here, we apply a viscosity range of 8 orders of magnitude. However, for the majority of models, the viscosity profile stays well within the maximum and minimum cutoffs.

2.3 Lithosphere scarring

In the modelling of a mantle suture, we specify an inherited plane of weakness that has remained over a long period of time (in this case, since the Palaeoproterozoic). There are a number of mechanisms where a mantle lithosphere suture could remain weak over time [e.g., *Erdős et al.*, 2014; *Manatschal et al.*, 2015; *Petersen and Schiffer*, 2016; *Heron et al.*, 2018], one of which is through grain size reduction of peridotite mylonites at ancient plate boundaries [*Bercovici and Ricard*, 2014]. The mantle lithosphere scar modeled here is 10 km thick, dipping at an angle of 45^o from the horizontal from 32 km depth down to 52 km (Figure 3a), and rheologically weak by having a reduced angle of internal friction compared to the surrounding material (Table 1). Due to the lack of high resolution geophysical imaging at depth in the region, there is uncertainty in the dip of a mantle structure (or even if there is a heterogeneity present). However, the influence of changing shape and dip angle of generic styles of such weak scars is explored in detail in *Heron and Pysklywec* [2016]; *Jourdon et al.* [2017]; *Salazar-Mora et al.* [2018]; *Heron et al.* [2019], and additional models shown in the Supplementary Information.

2.4 Extension rate and boundary conditions

Figure 4 shows the velocity azimuth and magnitude for the Davis Strait using plate reconstruction histories [*Seton et al.*, 2012] and the GPlates software [*Müller et al.*, 2018]. According to this reconstruction, between 200 and 120 Ma there was no significant extension between Greenland and Eastern Canada. During the early to mid-Cretaceous, extension initiates with an azimuth of approximately 40^o in present-day coordinates. However, it was not until the late-Mesozoic/early-Cenozoic that there was significant extension in the region. Thus, we identify a "Phase 1" between 75 Ma to 55 Ma as having an average extension velocity of 1 cm/yr at an azimuth of approximately 60^o. The azimuth of continental separation rotates anticlockwise in the Cenozoic (Figure 4a), and we identify therefore a "Phase 2" with a higher velocity magnitude at a high angle to the Phase 1 extension direction (Figure 4c). Following the work of *Peace et al.* [2018a], Phase 1 produced the rift shape alongside the spreading in the Labrador Sea and Baffin Bay. In this study, we focus on the initial stages of the rift system and investigate Phase 1 closely. Phase 2 is not thought to have significantly thinned the Davis Strait, although a number of strike-slip crustal features are due to this approximately NE-SW extensional activity [*Wilson et al.*, 2006].

To model Phase 1 (Figure 4c), we apply a prescribed boundary velocity on the north and south boundaries, and tangential velocity boundary conditions on the west, east, and base walls of the model, and a free surface on top [*Rose et al.*, 2017]. We have modelled the Cartesian 3-D box large enough so that deformation driven from the scarring is not influenced by the tangential boundary conditions (as described below).

The prescribed boundary condition on the north wall is a 0.5 cm/yr extension for the lithosphere (120 km) and a return flow of -0.3 cm/yr for the bottom 200 km of the box. In between, the velocity tapers from 0.5 cm/yr to 0 cm/yr from 120 km to 225 km depth, and from 0 cm/yr to -0.3 cm/yr from 200 km to 400 km depth. The reverse is applied to the west wall, with 0.5 cm/yr extension for the lithosphere. After extensive testing, we found this velocity profile as a boundary condition to provide stable solutions while maintaining mass balance (meaning no additional mass is added to the box). This prescribed boundary velocity produces an extension rate of 1 cm/yr in the lithosphere. This falls within the appropriate velocity magnitude as given in Figure 4.

The free surface allows topography to form and is formulated using an Arbitrary Lagrangian-Eulerian (ALE) framework for handling motion of the mesh (for more details please refer to *Rose et al.* [2017]). All of the calculations presented here have ~5,500,000 free surface degrees of freedom.

2.5 Thermal model setup

An initial temperature field is prescribed (Figure 3a) but is allowed to evolve during the simulation. The initial temperature follows a typical continental geotherm [*Chapman*, 1986] with no lateral variations. Our initial condition models the late-Mesozoic extension of two continental blocks, which collided in the Palaeoproterozoic (Fig 2). Therefore, the closure of the oceanic basin to accrete northern Greenland to the North Atlantic Craton occurred >1 Gyr in the past, and therefore there are no remaining thermal perturbations from that tectonic event. The temperature equation for calculating the initial geotherm is given as follows:

$$T(z) = T_o + \frac{q}{k}z - Hz^2/2k, \tag{7}$$

where T_o is the temperature at the top of the specific layer, H is the heat production, q is the heat flow through the surface of the specific layer, k is the thermal conductivity, and z is the depth. Table S1 gives the values for the thermal constraints required to generate the geotherm. As described in *Naliboff and Buiter* [2015], we use a high conductivity in the asthenosphere to maintain the high adiabat in the layer, and to generate a constant heat flux into the lithosphere [*Pysklywec and Beaumont*, 2004].

3 Results

Below, we present numerical models of continental extension in the presence of lithosphere inheritance related to West Greenland.

3.1 Crustal inheritance and mantle inheritance

Figure 5 shows the impact of crustal and mantle lithosphere inheritance on the evolution of the Davis Strait. To test the applicability of crustal inheritance in generating the first order tectonics as seen in the Davis Strait, we apply in Model C1 a crustal fault from previous geological studies [*van Gool et al.*, 2002; *Wilson et al.*, 2006; *Peace et al.*, 2018a] that is similar in geometry to the Itertoq thrust zone (ITZ) (Figure 2 and 5a). After 15 Myr of E-W extension, the surface strain rate in Model C1 indicates that the inheritance does not localize in the region of the scar (Figure 5b). The rifting pattern does not gen-

erate the relevant tectonic features, as outlined in the four-point checklist for the Davis Strait.

Model CM1 shows the rifting pattern across the region after 15 Myr of extension in the presence of the crustal scars in Model C1 and a mantle lithosphere inherited structure (Figure 5a). The mantle lithosphere scar represents the Nagssugtoqidian suture separating the North Atlantic craton from the continental material to the north (Figure 3b). In Model CM1, the strain rate replicates the right-stepping segmentation of the rifted conjugate margins (Figure 5b), with the upper crustal tectonics at 15 Myr producing spreading in the north and south of the model and preserving continental material across the oblique section of the suture (Figure 5c). As a result, Model CM1 meets the four-point checklist for the rift and ocean basin architecture.

In Model M1, the crustal inheritance from CM1 is removed, yet there is little difference in the evolution of the rift system (Figure 5). In this instance, the tectonics of the region are dominated by the mantle lithosphere structure. Applying only crustal inheritance that mimics the shape of the Nagssugtoqidian suture (e.g., a shallower scar as used in Model M1) is shown in Model C2 (Figure 5a). The tectonic evolution of the region is very different as compared to the similar Model M1. In Model C2, the southern limb of the suture begins to spread and propagates north-south (Figure 5c). Reapplying the mantle lithosphere suture in Model CM2 (Figure 5a) dominates the evolution of the region, as previously shown in Model CM1.

3.2 Evolution of the rift

Figure 6 shows the rift evolution of the reference Model M1, which enables an interpretation of what is occurring to reproduce the appropriate tectonic patterns of the Davis Strait. The surface strain rate pattern in Figure 6a shows an initial reactivation of the southern limb (A) and the oblique portion of the scar (B) at depth generates localized deformation in the crust. After 4 Myr of extension, there is little activity in the north of the model. However, after 7 Myr, the surface strain rate pattern indicates a localization of deformation to the north of the mantle suture (C, Figure 6a). The eastern limb of the suture does not appear to reactivate.

The thinning and spreading of the upper crust is shown in Figure 6b, with spreading developing first in the south (12 Myr) and then in the north (14 Myr) which is in keeping with geological interpretations of Labrador sea and Baffin Bay [*Peace et al.*, 2018a, 2017; *Seton et al.*, 2012]. There remains a region between the north and south spreading regions that is preserved, but thinned, continental material, which we describe as being a modelled Davis Strait.

The mantle lithosphere suture plays a significant role in the development of the southern "Labrador Sea" rift - the southern limb of the structure is perpendicular to the extension direction and as such facilitates the rifting and spreading (Figure 6b, A). However, the oblique portion of the scar transmits strain across it (Figure 6a, B), but the locus of extension diverts to being perpendicular to the extension direction once the mantle scar changes orientation to E-W (Figure 6a, C).

3.3 The complexity of obliquity

Figure 7 explores the potential role of obliquity in controlling the rifting pattern. The reference setup for Model M1 has a 45^o angle from the extension axis for the oblique portion of the mantle lithosphere suture. In Figure 7, this angle is changed to be less acute (M70, M65) or more acute (M40, M20) to gauge the range of obliquity at which the reference model can still produce Davis Strait tectonics. For Models M70 and M65, the acute angle cannot maintain the full four-point checklist as a right step segmentation is not

generated. However, a narrow region of preserved continental material is still produced (Figure 7).

Decreasing this angle of obliquity in M40 (40^o angle from the extension axis for the oblique portion of the mantle lithosphere suture) maintains the four-point checklist. However, a 20^o obliquity to extension direction mantle suture (Model M20) is not able to propagate strain across it and a north-south rift pattern is produced (Figure 7).

Figure 7 further highlights the importance of this oblique portion of the mantle suture in Model M1wide and M1gap. In M1wide, the width of the oblique section is increased (with an angle of 45^o) and still allows strain to propagate across it. Indeed, the spacing between the north and south spreading regions is increased compared to Model M1 (Figure 7). However, if we remove the oblique portion from M1 altogether (e.g., Model M1gap), we produce north-south spreading. The ability of the suture to transmit strain across the oblique portion is paramount to developing the appropriate rift and ocean basin architecture (Figure 7).

3.4 Model comparison with gravity data

For the models presented that satisfy the four-point tectonic checklist (e.g., CM1, M1, CM2, M40, M1wide), the surface evolution of the models is encouraging (Figure 6). However, it is important to compare the results of the numerical models with independent estimates of sub-surface structure. Figure 8 shows cross-sections of Model M1 after 15 Myr for north and south sections of the rift, as well as across the Davis Strait (lines given in Figure 6c).

The rifting dynamics across the model changes significantly from north to south. In the south of the model, the spreading occurs asymmetrically (Figure 8c), with more pronounced necking to the west of the spreading centre. However, in the north (Figure 8a), the rift is more symmetric. The pre-existing angled mantle suture promotes this asymmetry in the south, whereas in the north the rift propagates without any inherited features. It appears that in the north the spreading occurs as a result of being perpendicular to the extension direction (Figure 6).

Figure 9a shows a subset of Figure 8b, and shows the thinned Davis Strait with variable topography. Figure 9b shows a gravity inversion giving the depth to Moho for the region (as described in the Supplementary Material and *Welford and Hall* [2013]; *Welford et al.* [2018]). Across the Davis Strait we see some areas of shallow Moho towards Greenland in the east (circled in red). This corresponds to the thinning of the crust across our model Davis Strait (circled in red, Figure 9a). Furthermore, our model could produce decompression melting related to the thin mantle lithosphere as outlined in Figure 9a. It is understood that melting occurred during the Paleogene across the Davis Strait [*Larsen et al.*, 2009]. Our angled and thinned mantle lithosphere could be a pathway for such decompression melting patterns, and as a result a potential site of magmatic underplating.

4 Discussion

Results from our modelling show the impact of mantle lithosphere scarring related to a Palaeoproterozoic orogenic event in the development of the complex Mesozoic-Cenozoic rifting and ocean basin formation between Greenland and Canada (Figure 5), and highlight the potential role of obliquity in the rift evolution (Figure 7). Although a number of studies have previously modelled oblique rifting in three-dimensions [*Brune et al.*, 2014; *Zwaan et al.*, 2016; *Brune et al.*, 2017; *Farangitakis et al.*, 2019], our study shows tectonic features related to West Greenland and offers a new geodynamic explanation for the Phanerozoic rift event in the region.

4.1 Mechanism

Figure 10 outlines a mechanism for the evolution of the Davis Strait during the Paleocene. First, in the region of the present-day Labrador Sea, there is a reactivation of a mantle lithosphere suture related to the accretion of the North Atlantic Craton. The suture, outlined in green as given by *van Gool et al.* [2002], in this region is perpendicular to the extension direction generated by the plate motion in the late Paleocene/early Eocene [*Seton et al.*, 2012]. The model rifting first to the south of the Davis Strait follows the geological history of the region, with Labrador Sea spreading occurring before Baffin Bay spreading in the north [*Peace et al.*, 2017; *Abdelmalak et al.*, 2018].

The middle panel of Figure 10 shows the angled portion of the suture that connects the Nain Province (NP) and how the north of the North Atlantic Craton plays an important role in the evolution of the Davis Strait (grey region). The obliquity of the suture to the late Paleocene extension direction does not permit the Davis Strait to achieve breakup in the same way as in the Labrador Sea. Although our model Davis Strait undergoes extensive thinning (transtension) (Figure 8), the oblique suture delays, and ultimately prohibits spreading. Stress is transmitted across the oblique suture, creating the elevated region that becomes the Davis Strait.

This stress transfer follows the mantle suture until it becomes parallel to the extension direction on Greenland (Figure 10). Despite the presence of a weak region of mantle lithosphere in the east of the model, the rift propagates north perpendicular to the extension direction into the Baffin Bay region (Figure 6). In our models there is no structural inheritance to the north of our Davis Strait; because of this, the Labrador Sea and Baffin Bay spreading patterns are very different (Figure 9a).

4.2 The influence of the mantle lithosphere in tectonic processes

It has been noted by many workers that the Mesozoic rifting and Cenozoic margin and basin formation in West Greeland cross-cuts basement orogenic belts and cratons [e.g., *Larsen and Rex*, 1992; *Tappe et al.*, 2007; *Buiter and Torsvik*, 2014] and in particular the North Atlantic Craton was split by the Labrador Sea, meaning a thin sliver is now located to the west in the Torngat region on Labrador (see Fig 1). This cross-cutting relationship prompts the question as to why the Labrador Sea ocean basin opened where it did and not further west at the surface in the Torngat Palaeoproterozoic belts? A possible answer provided by this study is that an east-dipping Palaeoproterozoic suture (Fig 2) would have been located at mantle depths many tens of kilometers inboard of the surface trace of the western margin of the North Atlantic Craton. If this mantle feature localized extensional strain in the crust directly above, as demonstrated by our models, then it would be entirely feasible that a strip of the North Atlantic Craton could end up on the Labrador side of the newly formed ocean basin (Fig 1). Indeed, this provides a mechanism by which structural inheritance by unseen mantle structures influences upper crustal deformation patterns and creates crustal slivers, in this case promoting cross-cutting narrow margins by necking of the overlying crust [e.g., *Wenker and Beaumont*, 2018], where the extension direction is perpendicular to the pre-existing mantle scar.

The Palaeoproterozoic Nagssugtoqidian orogenic belt to the north of the North Atlantic Craton was first identified as a persistent (>2.5 Gyrs) tectonic lineament by *Watterson* [1975], who regarded the boundary as a lithosphere-scale structure due to the presence of Cambrian age kimberlites that are cross-cut by Mesozoic age pseudotachylytes [*Grocott*, 1977]. Subsequent investigation of brittle deformation in exposures of the Nagssugtoqidian Orogen adjacent to the Davis Strait by *Wilson et al.* [2006] revealed a two-phase model for fault development that is compatible with the development of the Mesozoic to Cenozoic continental margin offshore [*Chalmers et al.*, 1993; *Oakey and Chalmers*, 2012]. *Wilson et al.* [2006] found that the Phase 1 generally N-S trending normal faults were compatible with the opening of the Labrador Sea - Davis Strait - Baffin Bay seaway in the

Early Cretaceous to Paleocene. Phase 2 faults are strike-slip and thrust structures that are spatially confined to ductile shear zones within the Nagssugtoqidian (such as the Norder Isortoq shear zone, Fig 2) and explained by partitioning of the wrench deformation that formed the Eocene Ungava transform system (via pre-existing structures) [*Wilson et al.*, 2006].

The main Palaeoproterozoic shear zones identified as part of the Nagssugtoqidian Orogen continue offshore and control the primary depocentres and later transpressional deformation in the Davis Strait region [*Wilson et al.*, 2006; *Peace et al.*, 2017]. Early Cretaceous syn-rift fault patterns show generally margin parallel NNW-SSE trends in Labrador Sea and Baffin Bay, however in the Davis Strait region the faults show a broad, diffuse pattern with the main faults rotated clockwise relative to the overall margin trend [*Chalmers et al.*, 1993; *Oakey and Chalmers*, 2012; *Alsulami et al.*, 2015; *Peace et al.*, 2017]. This pattern is compatible with the Davis Strait forming as a zone of transtensional deformation, under local ENE-WSW extension in a right-stepping transfer zone from Labrador Sea into Baffin Bay. In this scenario the Davis Strait was a primary structure formed prior to the change in spreading direction in the Eocene. The coincidence of the Davis Strait transtensional zone with the offshore continuation of the Nagssugtoqidian orogenic shear zones led *Wilson et al.* [2006] to suggest that deformation was 'strongly influenced by basement fabrics such that this region experienced complex 3-D strain'. We now suggest this crustal inheritance, which is clearly expressed in the fault patterns, the depositional history of the basins and the overall crustal thickness [*Welford et al.*, 2018], was in effect a passive response to the oblique deformation controlled by the mantle scar beneath. The overall right step of the margin, which set up the oblique extensional deformation zone which becomes the Davis Strait was a first order response to the locus of stretching deformation seeking to follow the mantle scar where it was oblique to the stretching direction. Further east, where the mantle scar becomes perpendicular to the overall stretching direction is the point (south end of Baffin Bay) where the locus of deformation resumed its NNW-SSE direction.

This study presents a new, deep origin of the inheritance that may drive deformation in a region where only crustal processes have previously been suggested [*Wilson et al.*, 2006; *Peace et al.*, 2018a,b]. It should be noted that it is indeed unexpected that applying a North Atlantic Craton mantle suture (Figure 3b) in the presence of an extension field that is relevant in velocity and orientation to the Paleogene (Figure 4) would produce appropriate rift dynamics for the Davis Strait system (Figure 6). However, the study here complements a growing body of work that highlights the potential of the mantle lithosphere to play an important role in tectonic processes [*Pysklywec and Beaumont*, 2004; *Babuška and Plomerová*, 2013; *Heron et al.*, 2016; *Jourdon et al.*, 2017; *Salazar-Mora et al.*, 2018; *Phillips et al.*, 2018; *Balázs et al.*, 2018; *Heron et al.*, 2019].

4.3 3-D modelling

We present 3-D numerical models that are 800 km × 800 km and have a crustal resolution of 1 km. There are distinct advantages to using such models over 2-D simulations, as discussed in *Le Pourhiet et al.* [2018]. However, there are drawbacks related to these higher dimension models. For instance, due to computational expense, we are unable to model dynamically the full evolution of the region. That is, simulate the continental collision that produced the Nagssugtoqidian Orogen and subsequent hypothesized mantle lithosphere sutures in the Palaeoproterozoic, then organically generate the Mesozoic-Cenozoic rifting as a result of far-field plate motion [e.g., *Naliboff and Buiter*, 2015; *Salazar-Mora et al.*, 2018].

By manually implementing such a mantle scar as an initial condition we negate a lot of the geological history of the region. However, our hypothesis that ancient tectonic activity could produce weak lithospheric structures that remain dormant over long timescales

before reactivation is well established [e.g., *Vauchez et al.*, 1997; *Holdsworth et al.*, 2001]. Indeed, this study is important as it applies well established theories regarding mantle lithosphere inheritance [e.g., *Bercovici and Ricard*, 2014] to a regional geological feature. Here, a mantle lithosphere structure can generate appropriate deformation related to the Davis Strait and follows a number of previous studies highlighting the importance of the mantle lithosphere in tectonic processes [e.g., *Vauchez et al.*, 1997; *Pysklywec and Beaumont*, 2004; *Babuška and Plomerová*, 2013; *Hopper and Fischer*, 2015; *Heron et al.*, 2015; *Petersen and Schiffer*, 2016; *Heron et al.*, 2016; *Heron and Pysklywec*, 2016; *Jourdon et al.*, 2017; *Phillips et al.*, 2018; *Balázs et al.*, 2018; *Salazar-Mora et al.*, 2018; *Heron et al.*, 2019].

The plate motion, which we apply here as a boundary condition, is an important part of the history of the region. Figure 4 shows the relative velocities and orientation of the plate motion over the course of the rift [*Seton et al.*, 2012]. In our modelling, we have fixed the extension velocity and orientation for 15 Myr in order to approximate Phase 1 of the rift history (Figure 4). Our modelled Davis Strait region is susceptible to rifting and indeed thins throughout the simulation, which is in keeping with geophysical interpretation of the region (Figure 9b) [*Funck et al.*, 2007; *Suckro et al.*, 2013]. If we allow our reference case Model M1 to deform for longer than 15 Myr, the modelled Davis Strait thins further before joining up to the north and south spreading zones after 19 Myr (Fig. S5).

Due to numerical complexity and computational expense, it is difficult to apply a time-dependent extension velocity covering the whole rift sequence (Figure 4). However, the extension velocity and orientation used here fall within the estimation for Phase 1. As outlined in *Peace et al.* [2018a] (and shown in Figure 1b), the four-point checklist for the rift evolution of the region has already been satisfied at the end of Phase 1 (60 Ma, 15-20 Myr after extension is initiated). The rotation of the extension axis to approximately north-south in Phase 2 (Figure 4) has an impact on the fault orientation and kinematics but not on the overall geometry of breakup [*Peace et al.*, 2018a]. As a result, modelling only Phase 1 (e.g., 1 cm/yr at 15 Myr) is appropriate for our study.

4.4 Parameter analysis

In testing the robustness of our study we explored the parameter space surrounding these 3-D numerical models of extension of continental lithosphere finding that the choice of rheological parameters is important to the development of appropriate Davis Strait tectonics. *Schiffer et al.* [2016] interpret mantle lithosphere scarring on the continental margin of East Greenland to be of higher density than the surrounding mantle material, with *Petersen and Schiffer* [2016] providing modelling on the topic. In our study, through changing our mantle lithosphere scar from an area of weakness to being stronger than the surrounding material, we were unable to produce any focusing of strain that would allow a Davis Strait-type geometry rift to develop. However, a number of studies have discussed the weakening impact of tectonic processes on the lithosphere to facilitate continental rifting [*Dunbar and Sawyer*, 1988, 1989]. The subduction of crustal material into the mantle through ancient processes could increase volatiles to the lower lithosphere, weakening the seismically imaged scarred material [*Pollack*, 1986; *Petersen and Schiffer*, 2016].

We also studied the strain range over which material is weakened (e.g., Fig. S3). In Models M2 - M5 we used Model M1 setup and changed the strain range for weakening to different values used in recent studies [e.g., *Huismans and Beaumont*, 2011; *Brune et al.*, 2013; *Naliboff and Buiter*, 2015; *Salazar-Mora et al.*, 2018]. We found some differences between the results with regards to the evolution of the rift (e.g., Figs. S3 and S4), however they all satisfied the required four-point checklist for Davis Strait tectonics (Fig. S3). Although the parameters used in the main manuscript are in keeping with the rest of the community [e.g., *Brune et al.*, 2017], the work presented here highlights the difficulty of

modelling strain weakening due to the unconstrained nature of the values for different rheologies.

5 Conclusions

For the first time, numerical simulations show that rifting of lithosphere with a pre-existing mantle structure can reproduce first order features that resemble the Labrador Sea, Davis Strait, Baffin Bay continental margins and ocean basins (Figure 6). The results offer a new mechanism for rifting in the region, focusing on the role of ancient mantle lithosphere suturing rather than or in addition to crustal inheritance (Figure 5). The obliquity of the suture to the extension direction is important for the tectonic evolution of the region, and generates a segmented rift pattern (Figure 7). This study supplements a growing body of work that is posing questions on the fundamentals of inheritance, and shows that we should be looking deeper than the Moho for controls on the tectonic style of lithosphere-scale deformation.

Acknowledgments

P.J. Heron is grateful for funding from the European Union's Horizon 2020 research and innovation program under the Marie Sklodowska-Curie grant agreement 749664. A. L. Peace gratefully acknowledges support from the Hibernia project Geophysics Support Fund at Memorial University of Newfoundland and from Innovate NL. R.N. Pysklywec acknowledges support from a Natural Sciences and Engineering Research Council of Canada Discovery Grant and an allocation with ComputeCanada. J.K. Welford also acknowledges support from a Natural Sciences and Engineering Research Council of Canada Discovery Grant. Computations were performed on the Niagara supercomputer at the SciNet HPC Consortium. SciNet is funded by: the Canada Foundation for Innovation; the Government of Ontario; Ontario Research Fund - Research Excellence; and the University of Toronto. We thank the Computational Infrastructure for Geodynamics (geodynamics.org) which is funded by the National Science Foundation under award EAR-0949446 and EAR-1550901 for supporting the development of ASPECT. Data will be made available from the authors (as outlined in the supporting information).

References

Abdelmalak, M., L. Geoffroy, J. Angelier, B. Bonin, J. Callot, J. Gélard, and C. Aubourg (2012), Stress fields acting during lithosphere breakup above a melting mantle: A case example in West Greenland, *Tectonophysics*, *581*, 132 – 143, doi: https://doi.org/10.1016/j.tecto.2011.11.020, crustal Stresses, Fractures, and Fault Zones: The Legacy of Jacques Angelier.

Abdelmalak, M., S. Planke, S. Polteau, E. Hartz, J. Faleide, C. Tegner, D. Jerram, J. Millett, and R. Myklebust (2018), Breakup volcanism and plate tectonics in the NW Atlantic, *Tectonophysics*, doi:10.1016/j.tecto.2018.08.002.

Alsulami, S., D. Paton, and D. Cornwell (2015), Tectonic variation and structural evolution of the West Greenland continental margin, *AAPG Bulletin*, *99*(09), 1689–1711, doi:10.1306/03021514023.

Amante, C., and B. W. Eakins (2009), ETOPO1 1 Arc-Minute Global Relief Model: NOAA Technical Memorandum NESDIS Procedures, *Data Sources and Analysis*, *NGDC-24*.

Babuška, V., and J. Plomerová (2013), Boundaries of mantle–lithosphere domains in the Bohemian Massif as extinct exhumation channels for high-pressure rocks, *Gondwana Research*, *23*(3), 973 – 987, doi:https://doi.org/10.1016/j.gr.2012.07.005, ultrahigh-pressure and high-pressure metamorphic terranes in orogenic belts: reactions, fluids and geological processes.

Balázs, A., L. Matenco, K. Vogt, S. Cloetingh, and T. Gerya (2018), Extensional Polarity Change in Continental Rifts: Inferences From 3-D Numerical Modeling and Observations, *Journal of Geophysical Research: Solid Earth*, *123*(9), 8073–8094, doi:10.1029/2018JB015643.

Bangerth, W., J. Dannberg, R. Gassmöller, T. Heister, et al. (2018a), ASPECT: Advanced Solver for Problems in Earth's ConvecTion, User Manual, doi:10.6084/m9.figshare.4865333, doi:10.6084/m9.figshare.4865333.

Bangerth, W., J. Dannberg, R. Gassmoeller, T. Heister, et al. (2018b), ASPECT v2.0.1 [software], doi:10.5281/zenodo.1297145.

Bercovici, D., and Y. Ricard (2014), Plate tectonics, damage and inheritance, *Nature*, *508*(7497), 513–516, doi:10.1038/nature13072.

Biryol, C. B., L. S. Wagner, K. M. Fischer, and R. B. Hawman (2016), Relationship between observed upper mantle structures and recent tectonic activity across the Southeastern United States, *Journal of Geophysical Research: Solid Earth*, *121*(5), 3393–3414, doi:10.1002/2015JB012698.

Bos, B. (2002), Frictional-viscous flow of phyllosilicate-bearing fault rock: Microphysical model and implications for crustal strength profiles, *Journal of Geophysical Research*, *107*(B2), doi:10.1029/2001jb000301.

Brune, S., A. A. Popov, and S. V. Sobolev (2013), Quantifying the thermo-mechanical impact of plume arrival on continental break-up, *Tectonophysics*, *604*, 51 – 59, doi:https://doi.org/10.1016/j.tecto.2013.02.009, progress in understanding the South Atlantic margins.

Brune, S., C. Heine, M. Pérez-Gussinyé, and S. V. Sobolev (2014), Rift migration explains continental margin asymmetry and crustal hyper-extension, *Nature Communications*, *5*, 4014 EP –.

Brune, S., C. Heine, P. D. Clift, and M. Pérez-Gussinyé (2017), Rifted margin architecture and crustal rheology: Reviewing Iberia-Newfoundland, Central South Atlantic, and South China Sea, *Marine and Petroleum Geology*, *79*, 257–281, doi:10.1016/j.marpetgeo.2016.10.018.

Buiter, S. J., and T. H. Torsvik (2014), A review of Wilson Cycle plate margins: A role for mantle plumes in continental break-up along sutures?, *Gondwana Research*, *26*(2), 627 – 653, doi:https://doi.org/10.1016/j.gr.2014.02.007.

Calvert, A. J., and J. N. Ludden (1999), Archean continental assembly in the southeastern Superior Province of Canada, *Tectonics*, *18*(3), 412–429, doi:10.1029/1999tc900006.

Calvert, A. J., E. W. Sawyer, W. J. Davis, and J. N. Ludden (1995), Archaean subduction inferred from seismic images of a mantle suture in the Superior Province, *Nature*, *375*(6533), 670–674, doi:10.1038/375670a0.

Chalmers, J. A., and T. Pulvertaft (2001), Development of the continental margins of the Labrador Sea: a review, *Geological Society, London, Special Publications*, *187*(1), 77–105, doi:10.1144/gsl.sp.2001.187.01.05.

Chalmers, J. A., T. C. R. PULVERTAFT, F. G. CHRISTIANSEN, H. C. LARSEN, K. H. LAURSEN, and T. G. OTTESEN (1993), The southern West Greenland continental margin: rifting history, basin development, and petroleum potential, *Geological Society, London, Petroleum Geology Conference series*, *4*(1), 915–931, doi:10.1144/0040915.

Chapman, D. S. (1986), Thermal gradients in the continental crust, *Geological Society, London, Special Publications*, *24*(1), 63–70, doi:10.1144/gsl.sp.1986.024.01.07.

Chian, D., C. Keen, I. Reid, and K. E. Louden (1995), Evolution of nonvolcanic rifted margins: New results from the conjugate margins of the Labrador Sea, *Geology*, *23*(7), 589, doi:10.1130/0091-7613(1995)023<0589:EONRMN>2.3.CO;2.

Clarke, D. B., and E. K. Beutel (2019), Davis Strait Paleocene picrites: Products of a plume or plates?, *Earth-Science Reviews*, doi:https://doi.org/10.1016/j.earscirev.2019.01.012.

Donea, J., and A. Huerta (2003), Finite Element Methods for Flow Problems, *John Wiley 'l&' Sons, Ltd*, doi:10.1002/0470013826.

649 Dunbar, J. A., and D. S. Sawyer (1988), Continental rifting at pre-existing lithospheric
650 weaknesses, *Nature*, *333*(6172), 450–452, doi:10.1038/333450a0.
651 Dunbar, J. A., and D. S. Sawyer (1989), How preexisting weaknesses control the
652 style of continental breakup, *Journal of Geophysical Research*, *94*(B6), 7278, doi:
653 10.1029/jb094ib06p07278.
654 Erdős, Z., R. S. Huismans, P. van der Beek, and C. Thieulot (2014), Extensional inheri-
655 tance and surface processes as controlling factors of mountain belt structure, *Journal of*
656 *Geophysical Research: Solid Earth*, *119*(12), 9042–9061, doi:10.1002/2014jb011408.
657 Farangitakis, G.-P., D. Sokoutis, K. J. W. McCaffrey, E. Willingshofer, L. M. Kalnins,
658 J. J. J. Phethean, J. van Hunen, and V. van Steen (2019), Analogue Modeling of Plate
659 Rotation Effects in Transform Margins and Rift-Transform Intersections, *Tectonics*, *38*,
660 doi:10.1029/2018TC005261.
661 Funck, T., H. R. Jackson, K. E. Louden, and F. Klingelhöfer (2007), Seismic study of the
662 transform-rifted margin in Davis Strait between Baffin Island (Canada) and Greenland:
663 What happens when a plume meets a transform, *Journal of Geophysical Research: Solid*
664 *Earth*, *112*(B4), doi:10.1029/2006jb004308.
665 Funck, T., K. Gohl, V. Damm, and I. Heyde (2012), Tectonic evolution of southern Baf-
666 fin Bay and Davis Strait: Results from a seismic refraction transect between Canada
667 and Greenland, *Journal of Geophysical Research: Solid Earth*, *117*(B4), n/a–n/a, doi:
668 10.1029/2011jb009110.
669 Gerlings, J., T. Funck, H. R. Jackson, K. E. Louden, and F. Klingelhöfer (2009), Seismic
670 evidence for plume-derived volcanism during formation of the continental margin in
671 southern Davis Strait and northern Labrador Sea, *Geophysical Journal International*,
672 *176*(3), 980–994, doi:10.1111/j.1365-246x.2008.04021.x.
673 Glerum, A., C. Thieulot, M. Fraters, C. Blom, and W. Spakman (2018), Nonlinear vis-
674 coplasticity in ASPECT: benchmarking and applications to subduction, *Solid Earth*,
675 *9*(2), 267–294, doi:10.5194/se-9-267-2018.
676 Grocott, J. (1977), The relationship between Precambrian shear belts and mod-
677 ern fault systems, *Journal of the Geological Society*, *133*(3), 257–261, doi:
678 10.1144/gsjgs.133.3.0257.
679 Grocott, J., and K. J. W. McCaffrey (2017), Basin evolution and destruction in an Early
680 Proterozoic continental margin: the Rinkian fold–thrust belt of central West Greenland,
681 *Journal of the Geological Society*, *174*(3), 453–467, doi:10.1144/jgs2016-109.
682 Heister, T., J. Dannberg, R. Gassmöller, and W. Bangerth (2017), High Accuracy Mantle
683 Convection Simulation through Modern Numerical Methods. II: Realistic Models and
684 Problems, *Geophysical Journal International*, *210*(2), 833–851, doi:10.1093/gji/ggx195.
685 Heron, P. J., and R. N. Pysklywec (2016), Inherited structure and coupled crust-mantle
686 lithosphere evolution: Numerical models of Central Australia, *Geophysical Research*
687 *Letters*, *43*(10), 4962–4970, doi:10.1002/2016gl068562.
688 Heron, P. J., J. P. Lowman, and C. Stein (2015), Influences on the positioning of man-
689 tle plumes following supercontinent formation, *Journal of Geophysical Research: Solid*
690 *Earth*, *120*(5), 3628–3648, doi:10.1002/2014jb011727.
691 Heron, P. J., R. N. Pysklywec, and R. Stephenson (2016), Lasting mantle scars
692 lead to perennial plate tectonics, *Nature Communications*, *7*, 11,834, doi:
693 10.1038/ncomms11834.
694 Heron, P. J., R. N. Pysklywec, and R. Stephenson (2018), Exploring the theory of plate
695 tectonics: the role of mantle lithosphere structure, *Geological Society, London, Special*
696 *Publications*, p. SP470.7, doi:10.1144/sp470.7.
697 Heron, P. J., R. N. Pysklywec, R. Stephenson, and J. van Hunen (2019), Deformation
698 driven by deep and distant structures: Influence of a mantle lithosphere suture in the
699 Ouachita orogeny, *Geology*, *47*(2), 147–150, doi:10.1130/G45690.1.
700 Hirth, G., and D. Kohlstedt (2003), Rheology of the upper mantle and the mantle wedge:
701 A view from the experimentalists, *Geophysical Monograph Series*, pp. 83–105, doi:
702 10.1029/138gm06.

Holdsworth, R. E., C. A. Butler, and A. M. Roberts (1997), The recognition of reactivation during continental deformation, *Journal of the Geological Society*, *154*(1), 73–78, doi:10.1144/gsjgs.154.1.0073.

Holdsworth, R. E., M. Stewart, J. Imber, and R. A. Strachan (2001), The structure and rheological evolution of reactivated continental fault zones: a review and case study, *Geological Society, London, Special Publications*, *184*(1), 115–137, doi:10.1144/gsl.sp.2001.184.01.07.

Hopper, E., and K. M. Fischer (2015), The meaning of midlithospheric discontinuities: A case study in the northern U.S. craton, *Geochemistry, Geophysics, Geosystems*, *16*(12), 4057–4083, doi:10.1002/2015gc006030.

Hosseinpour, M., R. D. Müller, S. E. Williams, and J. M. Whittaker (2013), Full-fit reconstruction of the Labrador Sea and Baffin Bay, *Solid Earth*, *4*(2), 461–479, doi:10.5194/se-4-461-2013.

Huismans, R., and C. Beaumont (2011), Depth-dependent extension, two-stage breakup and cratonic underplating at rifted margins, *Nature*, *473*, 74 EP –.

Jackson, H. R., C. E. Keen, R. K. H. Falconer, and K. P. Appleton (1979), New geophysical evidence for sea-floor spreading in central Baffin Bay, *Canadian Journal of Earth Sciences*, *16*(11), 2122–2135, doi:10.1139/e79-200.

Japsen, P., J. M. Bonow, J.-P. Peulvast, and R. W. Wilson (2006), Uplift, erosion and fault reactivation in southern West Greenland, *GEUS Field Reports*, *63*.

Jourdon, A., L. Le Pourhiet, C. Petit, and Y. Rolland (2017), The deep structure and reactivation of the Kyrgyz Tien Shan: Modelling the past to better constrain the present, *Tectonophysics*, doi:10.1016/j.tecto.2017.07.019.

Kachanov, L. M. (2004), Fundamentals of the Theory of Plasticity, *Dover Publications, Inc.*

Karato, S.-i. (2008), *Deformation of Earth Materials: An Introduction to the Rheology of Solid Earth*, Cambridge University Press, doi:10.1017/CBO9780511804892.

Karato, S.-i., and P. Wu (1993), Rheology of the Upper Mantle: A Synthesis, *Science*, *260*(5109), 771–778, doi:10.1126/science.260.5109.771.

Kerr, A., J. Hall, R. J. Wardle, C. F. Gower, and B. Ryan (1997), New reflections on the structure and evolution of the Makkovikian - Ketilidian Orogen in Labrador and southern Greenland, *Tectonics*, *16*(6), 942–965, doi:10.1029/97tc02286.

Kronbichler, M., T. Heister, and W. Bangerth (2012), High Accuracy Mantle Convection Simulation through Modern Numerical Methods, *Geophysical Journal International*, *191*, 12–29, doi:10.1111/j.1365-246X.2012.05609.x.

Larsen, L. M., and D. C. Rex (1992), A review of the 2500 Ma span of alkaline-ultramafic, potassic and carbonatitic magmatism in West Greenland, *Lithos*, *28*(3), 367 – 402, doi:https://doi.org/10.1016/0024-4937(92)90015-Q, potassic and ultrapotassic magmas and their origin.

Larsen, L. M., L. M. HEAMAN, R. A. CREASER, R. A. DUNCAN, R. FREI, and M. HUTCHISON (2009), Tectonomagmatic events during stretching and basin formation in the Labrador Sea and the Davis Strait: evidence from age and composition of Mesozoic to Palaeogene dyke swarms in West Greenland, *Journal of the Geological Society*, *166*(6), 999–1012, doi:10.1144/0016-76492009-038.

Le Pourhiet, L., N. Chamot-Rooke, M. Delescluse, D. A. May, L. Watremez, and M. Pubellier (2018), Continental break-up of the South China Sea stalled by far-field compression, *Nature Geoscience*, *11*(8), 605–609, doi:10.1038/s41561-018-0178-5.

Lie, J., and E. Husebye (1994), Simple-shear deformation of the Skagerrak lithosphere during the formation of the Oslo Rift, *Tectonophysics*, *232*(1), 133 – 141, doi:https://doi.org/10.1016/0040-1951(94)90080-9, seismic Reflection Probing of the Continents and their Margins.

Loken, C., D. Gruner, L. Groer, R. Peltier, N. Bunn, M. Craig, T. Henriques, J. Dempsey, C.-H. Yu, J. Chen, and et al. (2010), SciNet: Lessons Learned from Building a Power-efficient Top-20 System and Data Centre, *Journal of Physics: Conference Series*, *256*,

012,026, doi:10.1088/1742-6596/256/1/012026.

Manatschal, G., L. Lavier, and P. Chenin (2015), The role of inheritance in structuring hyperextended rift systems: Some considerations based on observations and numerical modeling, *Gondwana Research*, *27*(1), 140 – 164, doi: https://doi.org/10.1016/j.gr.2014.08.006.

Matthews, K. J., K. T. Maloney, S. Zahirovic, S. E. Williams, M. Seton, and R. D. Müller (2016), Global plate boundary evolution and kinematics since the late Paleozoic, *Global and Planetary Change*, *146*, 226–250, doi:10.1016/j.gloplacha.2016.10.002.

Mickus, K. L., and G. R. Keller (1992), Lithospheric structure of the south-central United States, *Geology*, *20*(4), 335, doi:10.1130/0091-7613(1992)020<0335:LSOTSC>2.3.CO;2.

Morgan, J., M. Hadwin, M. Warner, P. Barton, and R. Morgan (1994), The polarity of deep seismic reflections from the lithospheric mantle: Evidence for a relict subduction zone, *Tectonophysics*, *232*(1), 319 – 328, doi:https://doi.org/10.1016/0040-1951(94)90093-0, seismic Reflection Probing of the Continents and their Margins.

Müller, R. D., M. Seton, S. Zahirovic, S. E. Williams, K. J. Matthews, N. M. Wright, G. E. Shephard, K. T. Maloney, N. Barnett-Moore, M. Hosseinpour, and et al. (2016), Ocean Basin Evolution and Global-Scale Plate Reorganization Events Since Pangea Breakup, *Annual Review of Earth and Planetary Sciences*, *44*(1), 107–138, doi: 10.1146/annurev-earth-060115-012211.

Müller, R. D., J. Cannon, X. Qin, R. J. Watson, M. Gurnis, S. Williams, T. Pfaffelmoser, M. Seton, S. H. J. Russell, and S. Zahirovic (2018), GPlates: Building a Virtual Earth Through Deep Time, *Geochemistry, Geophysics, Geosystems*, *19*(7), 2243–2261, doi: 10.1029/2018GC007584.

Naliboff, J., and S. J. Buiter (2015), Rift reactivation and migration during multiphase extension, *Earth and Planetary Science Letters*, *421*, 58 – 67, doi: https://doi.org/10.1016/j.epsl.2015.03.050.

Oakey, G. N., and J. A. Chalmers (2012), A new model for the Paleogene motion of Greenland relative to North America: Plate reconstructions of the Davis Strait and Nares Strait regions between Canada and Greenland, *Journal of Geophysical Research: Solid Earth*, *117*(B10), doi:10.1029/2011jb008942.

Peace, A., K. McCaffrey, J. Imber, J. van Hunen, R. Hobbs, and R. Wilson (2018a), The role of pre-existing structures during rifting, continental breakup and transform system development, offshore West Greenland, *Basin Research*, *30*(3), 373–394, doi: 10.1111/bre.12257.

Peace, A., E. Dempsey, C. Schiffer, J. Welford, K. McCaffrey, J. Imber, and J. Phethean (2018b), Evidence for Basement Reactivation during the Opening of the Labrador Sea from the Makkovik Province, Labrador, Canada: Insights from Field Data and Numerical Models, *Geosciences*, *8*(8), 308, doi:10.3390/geosciences8080308.

Peace, A. L., G. R. Foulger, C. Schiffer, and K. J. McCaffrey (2017), Evolution of Labrador Sea–Baffin Bay: Plate or Plume Processes?, *Geoscience Canada*, *44*(3), 91–102, doi:10.12789/geocanj.2017.44.120.

Petersen, K. D., and C. Schiffer (2016), Wilson cycle passive margins: Control of orogenic inheritance on continental breakup, *Gondwana Research*, *39*, 131–144, doi: 10.1016/j.gr.2016.06.012.

Phillips, T. B., C. A.-L. Jackson, R. E. Bell, and O. B. Duffy (2018), Oblique reactivation of lithosphere-scale lineaments controls rift physiography – the upper-crustal expression of the Sorgenfrei–Tornquist Zone, offshore southern Norway, *Solid Earth*, *9*(2), 403–429, doi:10.5194/se-9-403-2018.

Pollack, H. N. (1986), Cratonization and thermal evolution of the mantle, *Earth and Planetary Science Letters*, *80*(1-2), 175–182, doi:10.1016/0012-821x(86)90031-2.

Pysklywec, R. N., and C. Beaumont (2004), Intraplate tectonics: feedback between radioactive thermal weakening and crustal deformation driven by mantle lithosphere instabilities, *Earth and Planetary Science Letters*, *221*(1), 275 – 292, doi:

https://doi.org/10.1016/S0012-821X(04)00098-6.

Roest, W. R., and S. P. Srivastava (1989), Sea-floor spreading in the Labrador Sea: A new reconstruction, *Geology*, *17*(11), 1000, doi:10.1130/0091-7613(1989)017<1000:sfsitl>2.3.co;2.

Rose, I., B. Buffett, and T. Heister (2017), Stability and accuracy of free surface time integration in viscous flows, *Physics of the Earth and Planetary Interiors*, *262*, 90 – 100, doi:10.1016/j.pepi.2016.11.007.

Rutter, E., and K. Brodie (2004), Experimental grain size-sensitive flow of hot-pressed Brazilian quartz aggregates, *Journal of Structural Geology*, *26*(11), 2011 – 2023, doi:https://doi.org/10.1016/j.jsg.2004.04.006.

Rybacki, E., M. Gottschalk, R. Wirth, and G. Dresen (2006), Influence of water fugacity and activation volume on the flow properties of fine-grained anorthite aggregates, *Journal of Geophysical Research: Solid Earth*, *111*(B3), n/a–n/a, doi:10.1029/2005jb003663.

Salazar-Mora, C. A., R. S. Huismans, H. Fossen, and M. Egydio-Silva (2018), The Wilson Cycle and Effects of Tectonic Structural Inheritance on Rifted Passive Margin Formation, *Tectonics*, *37*(9), 3085–3101, doi:10.1029/2018TC004962.

Schiffer, C., N. Balling, B. H. Jacobsen, R. A. Stephenson, and S. B. Nielsen (2014), Seismological evidence for a fossil subduction zone in the East Greenland Caledonides, *Geology*, *42*(4), 311–314, doi:10.1130/g35244.1.

Schiffer, C., N. Balling, J. Ebbing, B. H. Jacobsen, and S. B. Nielsen (2016), Geophysical-petrological modelling of the East Greenland Caledonides – Isostatic support from crust and upper mantle, *Tectonophysics*, *692*, 44 – 57, doi:https://doi.org/10.1016/j.tecto.2016.06.023, sI:Crustal seismology.

Schiffer, C., A. Peace, J. Phethean, L. Gernigon, K. McCaffrey, K. D. Petersen, and G. Foulger (2018), The Jan Mayen microplate complex and the Wilson cycle, *Geological Society, London, Special Publications*, p. SP470.2, doi:10.1144/sp470.2.

Scott, D. J. (1999), U–Pb geochronology of the eastern Hall Peninsula, southern Baffin Island, Canada: a northern link between the Archean of West Greenland and the Paleoproterozoic Torngat Orogen of northern Labrador, *Precambrian Research*, *93*(1), 5 – 26, doi:https://doi.org/10.1016/S0301-9268(98)00095-3.

Seton, M., R. Müller, S. Zahirovic, C. Gaina, T. Torsvik, G. Shephard, A. Talsma, M. Gurnis, M. Turner, S. Maus, and M. Chandler (2012), Global continental and ocean basin reconstructions since 200Ma, *Earth-Science Reviews*, *113*(3), 212 – 270, doi:https://doi.org/10.1016/j.earscirev.2012.03.002.

Srivastava, S. P. (1978), Evolution of the Labrador Sea and its bearing on the early evolution of the North Atlantic, *Geophysical Journal International*, *52*(2), 313–357, doi:10.1111/j.1365-246x.1978.tb04235.x.

St-Onge, M. R., J. A. M. Van Gool, A. A. Garde, and D. J. Scott (2009), Correlation of Archaean and Palaeoproterozoic units between northeastern Canada and western Greenland: constraining the pre-collisional upper plate accretionary history of the Trans-Hudson orogen, *Geological Society, London, Special Publications*, *318*(1), 193–235, doi:10.1144/sp318.7.

Steer, D. N., J. H. Knapp, and L. D. Brown (1998), Super-deep reflection profiling: exploring the continental mantle lid, *Tectonophysics*, *286*(1-4), 111–121, doi:10.1016/s0040-1951(97)00258-8.

Storey, M., R. Duncan, A. Pedersen, L. Larsen, and H. Larsen (1998), 40Ar/39Ar geochronology of the West Greenland Tertiary volcanic province, *Earth and Planetary Science Letters*, *160*(3-4), 569–586, doi:10.1016/s0012-821x(98)00112-5.

Suckro, S. K., K. Gohl, T. Funck, I. Heyde, B. Schreckenberger, J. Gerlings, and V. Damm (2013), The Davis Strait crust—a transform margin between two oceanic basins, *Geophysical Journal International*, *193*(1), 78–97, doi:10.1093/gji/ggs126.

Tappe, S., S. F. Foley, A. Stracke, R. L. Romer, B. A. Kjarsgaard, L. M. Heaman, and N. Joyce (2007), Craton reactivation on the Labrador Sea margins: 40Ar/39Ar age and Sr–Nd–Hf–Pb isotope constraints from alkaline and carbon-

atite intrusives, *Earth and Planetary Science Letters*, *256*(3), 433 – 454, doi: https://doi.org/10.1016/j.epsl.2007.01.036.

Thieulot, C. (2011), FANTOM: Two- and three-dimensional numerical modelling of creeping flows for the solution of geological problems, *Physics of the Earth and Planetary Interiors*, *188*(1), 47 – 68, doi:https://doi.org/10.1016/j.pepi.2011.06.011.

Thomas, W. A. (2006), Tectonic inheritance at a continental margin, *GSA Today*, *16*(2), 4, doi:10.1130/1052-5173(2006)016[4:tiaacm]2.0.co;2.

van Gool, J. A., J. N. Connelly, M. Marker, and F. C. Mengel (2002), The Nagssugtoqidian Orogen of West Greenland: tectonic evolution and regional correlations from a West Greenland perspective, *Canadian Journal of Earth Sciences*, *39*(5), 665–686, doi: 10.1139/e02-027.

Vauchez, A., G. Barruol, and A. Tommasi (1997), Why do continents break-up parallel to ancient orogenic belts?, *Terra Nova*, *9*(2), 62–66, doi:10.1111/j.1365-3121.1997.tb00003.x.

Vauchez, A., A. Tommasi, and G. Barruol (1998), Rheological heterogeneity, mechanical anisotropy and deformation of the continental lithosphere, *Tectonophysics*, *296*(1-2), 61–86, doi:10.1016/s0040-1951(98)00137-1.

Watterson, J. (1975), Mechanism for the persistence of tectonic lineaments, *Nature*, *253*(5492), 520–522, doi:10.1038/253520b0.

Welford, J. K., and J. Hall (2013), Lithospheric structure of the Labrador Sea from constrained 3-D gravity inversion, *Geophysical Journal International*, *195*(2), 767–784, doi: 10.1093/gji/ggt296.

Welford, J. K., A. L. Peace, M. Geng, S. A. Dehler, and K. Dickie (2018), Crustal structure of Baffin Bay from constrained three-dimensional gravity inversion and deformable plate tectonic models, *Geophysical Journal International*, *214*(2), 1281–1300, doi: 10.1093/gji/ggy193.

Wenker, S., and C. Beaumont (2018), Effects of lateral strength contrasts and inherited heterogeneities on necking and rifting of continents, *Tectonophysics*, *746*, 46–63, doi: 10.1016/j.tecto.2016.10.011.

Willett, S. D. (1992), *Dynamic and kinematic growth and change of a Coulomb wedge*, pp. 19–31, Springer Netherlands, Dordrecht, doi:10.1007/978-94-011-3066-0_2.

Wilson, J. T. (1966), Did the Atlantic Close and then Re-Open?, *Nature*, *211*(5050), 676–681, doi:10.1038/211676a0.

Wilson, R., K. E. S. Klint, J. A. M. van Gool, K. J. W. McCaffrey, R. E. Holdsworth, and J. A. Chalmers (2006), Faults and fractures in central West Greenland: Onshore expression of continental break-up and sea-floor spreading in the Labrador - Baffin Bay Sea, *Geological Survey of Denmark and Greenland Bulletin*.

Zwaan, F., G. Schreurs, J. Naliboff, and S. J. Buiter (2016), Insights into the effects of oblique extension on continental rift interaction from 3D analogue and numerical models, *Tectonophysics*, *693*, 239 – 260, doi:https://doi.org/10.1016/j.tecto.2016.02.036, special issue on Tectonics of oblique plate boundary systems.

960 **Table 1.** Rheological parameters for Model M1. For angle of internal friction and cohesion, strain weaken-
961 ing occurs over the range 0 to 0.5 [e.g., *Brune et al.*, 2017] and weakens by 50%. UC: upper crust; LC: lower
962 crust; ML: mantle lithosphere; A: asthenosphere; ML scar: mantle lithosphere scar.

Property	Unit	UC	LC	ML	A	ML Scar
Density	kg m^{-3}	2800	2900	3300	3300	3300
Thermal diffusivities	m^2 s^{-1}	1.905e-6	1.149e-6	1.333e-6	1.333e-6	1.333e-6
Viscosity prefactor	Pa^n m^{-p} s^{-1}	8.57e-28	7.13e-18	6.52e-16	6.52e-16	6.52e-16
Stress exponent		4.0	3.0	3.5	3.5	3.5
Activation energies	KJ mol^{-1}	223e3	345e3	530e3	530e3	530e3
Activation volumes	m^3 mol^{-1}	0	0	18e-6	18e-6	18e-6
Thermal expansivities	K^{-1}	2e-5	2e-5	2e-5	2e-5	2e-5
Specific heat	J kg^{-1} K^{-1}	750	750	750	750	750
Heat production	W m^{-3}	1.5e-6	0	0	0	0
Angles of internal friction	^{o}	20	20	20	20	0
Cohesions	Pa	20e6	20e6	20e6	20e6	20e6

963 **Table 2.** List of selected models in main manuscript (over 50 3-D models conducted). Checklist as outlined
964 in text.

Model	Checklist	Geometry	Figure
C1	1	Crustal scar setup 1	5
CM1	1,2,3,4	C1 plus mantle suture scar	5
M1	1,2,3,4	Mantle suture scar	5, 6, 8, 9
C2	1	Crustal scar setup 2	5
CM2	1,2,3,4	C2 plus mantle suture scar	5
M70	1,2,3,4	Oblique suture 75^o from x-axis	7
M65	1,2,3,4	Oblique suture 65^o from x-axis	7
M40	1,2,3,4	Oblique suture 40^o from x-axis	7
M20	1	Oblique suture 20^o from x-axis	7
M1wide	1,2,3,4	M1 with wider oblique suture	7
M1gap	1	M1 with no oblique suture	7

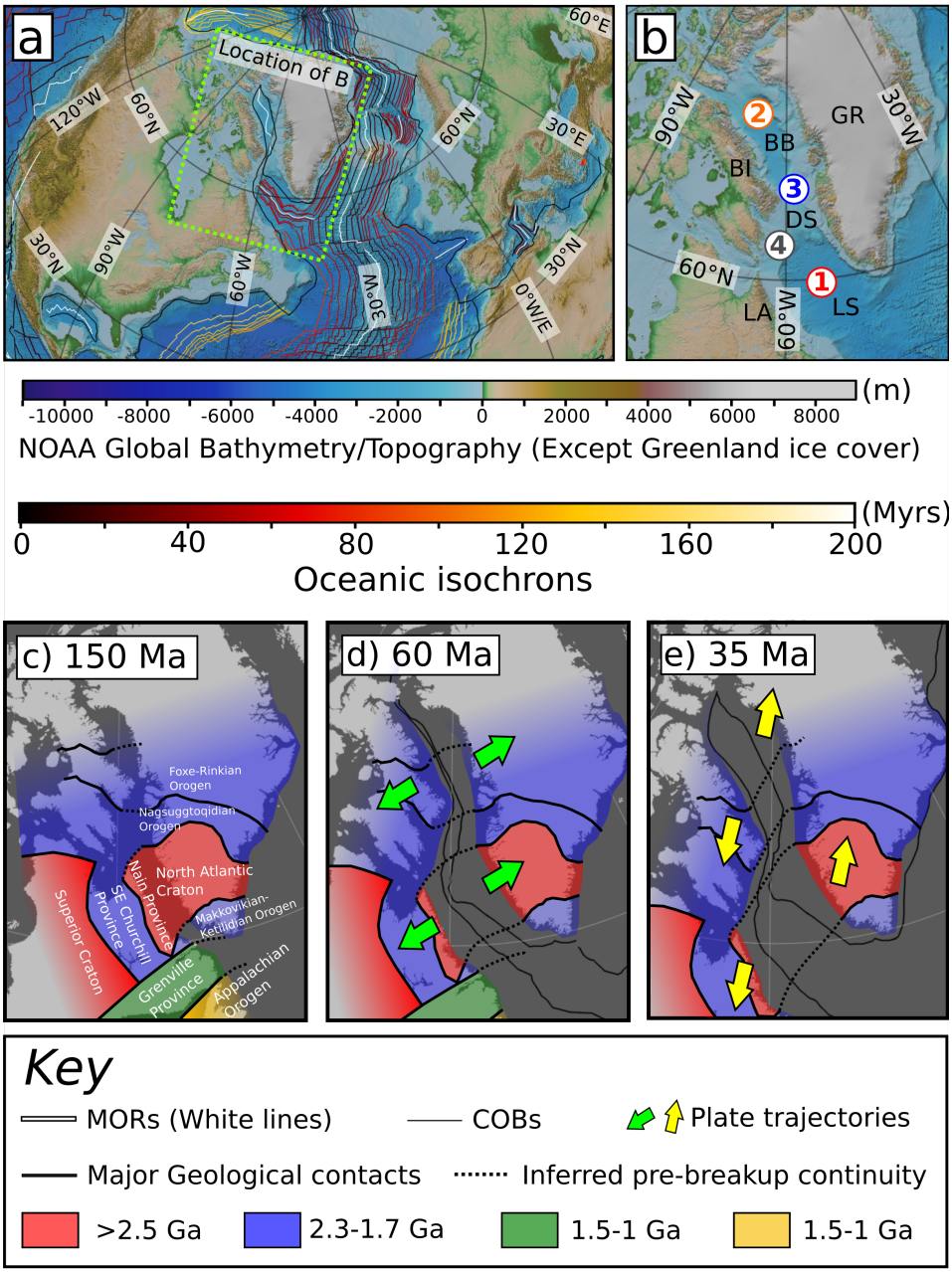

Figure 1. a) An overview of the North Atlantic spreading systems using the continent ocean boundaries and oceanic isochron compilations from *Müller et al.* [2016] plotted on top of the NOAA global bathymetry/topography model [*Amante and Eakins*, 2009]. b) Geographical overview of the NW Atlantic showing the key criteria that the model results are compared against. Abbreviations: BB = Baffin Bay, BI = Baffin Island, DS = Davis Strait, GR = Greenland, LA = Labrador and LS = Labrador Sea. c) Simplified overview of the basements that comprise the NW Atlantic borderlands in a pre-rifting and breakup configuration modified from *Kerr et al.* [1997] and *St-Onge et al.* [2009]. d-e) The NW Atlantic at 60 and 35 Ma, respectively, reconstructed using the model of *Matthews et al.* [2016] and shown with the calculated extensional directions from *Abdelmalak et al.* [2012].

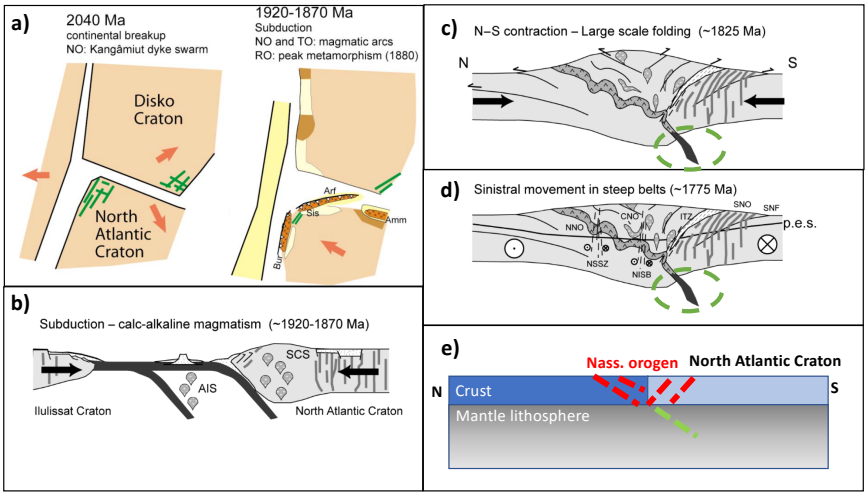

Figure 2. Tectonic history of the Nagssugtoqidian Orogen. (a) Plate outline of collision (modified from *van Gool et al.* [2002];) related subduction (b), collision (c) and movement to generate lithosphere scale deformation (d) (modified from *van Gool et al.* [2002]). Annotations: ISB, Itivdleq steep belt; ITZ, Ikertôq thrust zone; NISB, Nordre Isortoq steep belt; NSSZ, Nordre Strømfjord shear zone. SNF, southern Nagssugtoqidian front. CNO, NNO, and SNO are the central, northern, and southern Nagssugtoqidian Orogen, respectively. (e) We propose this deformation would leave a mantle scar (highlighted by dashed green lines in (c) and (d)). The ITZ is also the proposed location of the suture line in this orogen [*van Gool et al.*, 2002].

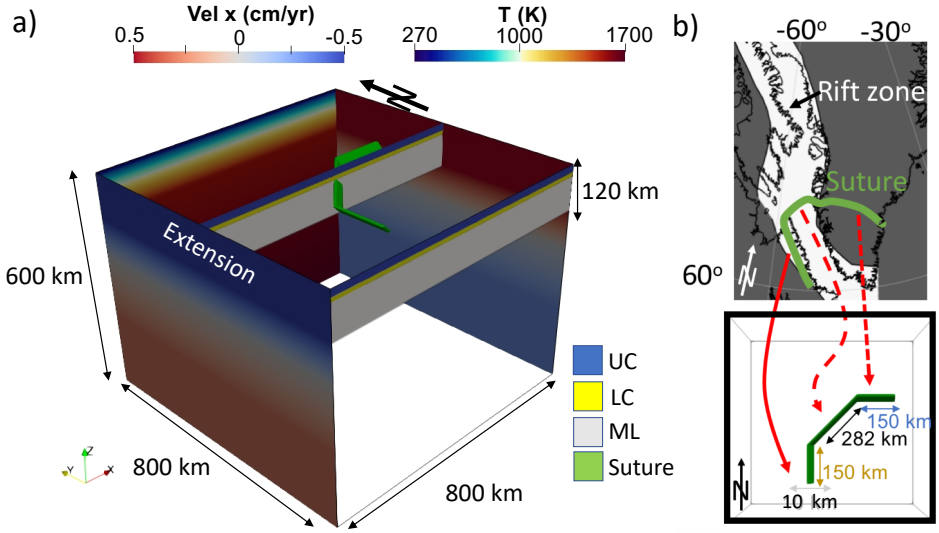

Figure 3. a) Initial setup of the numerical models presented here: 3-D box featuring crust, mantle lithosphere and a mantle scar with extension applied to the top 120 km (lithosphere) in a N-S direction, with outflow applied in the mantle below. East panel shows initial temperature profile across the whole box. b) Top panel shows a mantle scar delineating the outline of North Atlantic Craton suture. Bottom panel shows the model suture with three sections (south, oblique, and east) and their dimensions. The scar is applied as a zone of weakness (with a lower angle of internal friction than surrounding material).

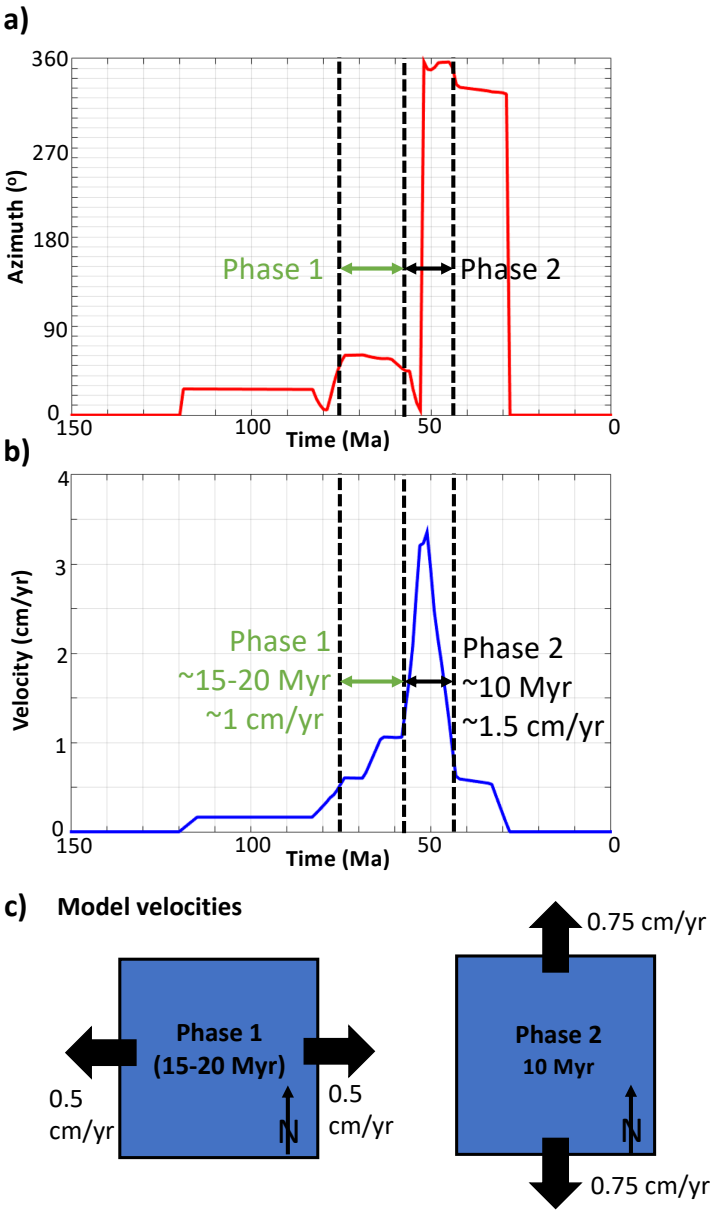

928 **Figure 4.** Calculated velocity azimuth (a) and magnitude (b) over time for the rift zone from the global
929 reconstruction compiled by *Seton et al.* [2012]. From these values we approximate the two phases of the rift
930 evolution (c).

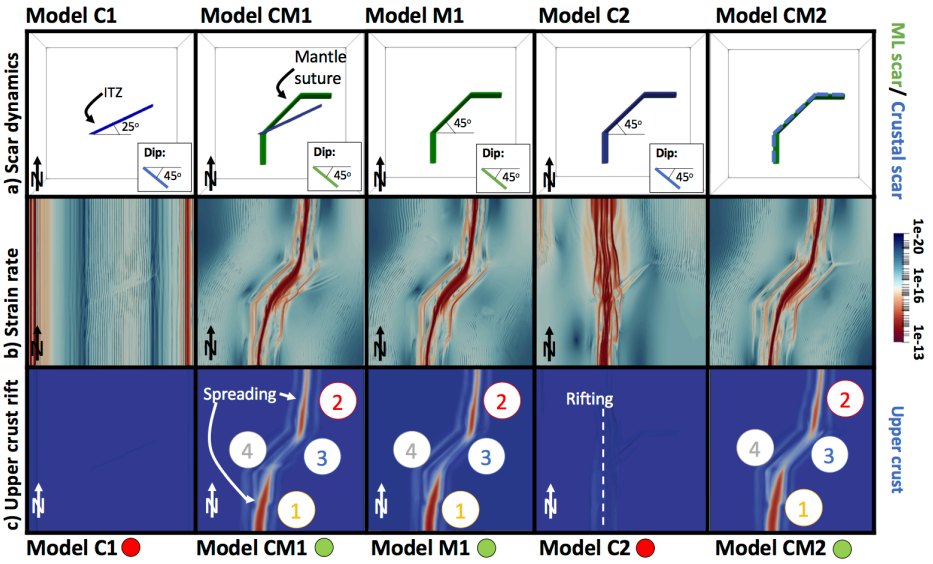

Figure 5. Rift dynamics for Model C1, CM2, M1, C2, and CM2 (Table 2). (a) Initial geometry of mantle lithosphere (green) and crustal (blue) scar. Surface strain rate (b) alongside upper crust (blue) and spreading position (red) (c) after 15 Myr. Annotation given as (1) rifting south of modelled Davis Strait to produce new oceanic crust; (2) rifting north of Davis Strait to produce new oceanic crust; (3) segmented rift geometry; and (4) preservation of the continental crust in the Davis Strait during extension. Green circle at base of figure indicates that model passed the four-point Davis Strait checklist and red circles indicate a negative result.

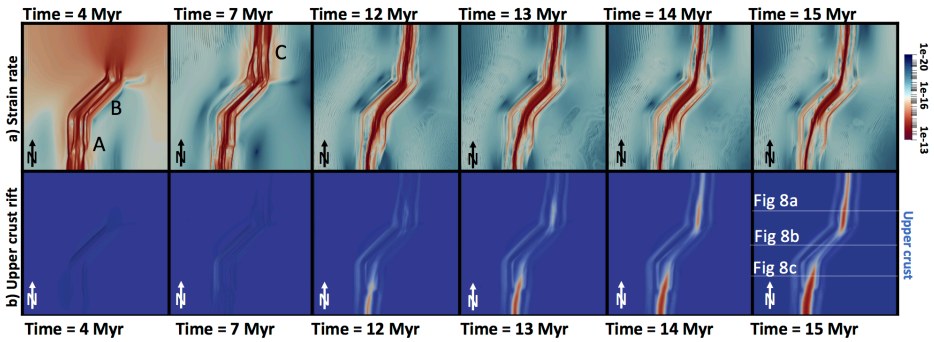

Figure 6. Time evolution of surface strain rate (a) alongside upper crust (blue) and spreading position (red) (c) after 4, 7, 12, 13, 14, and 15 Myr for Model M1.

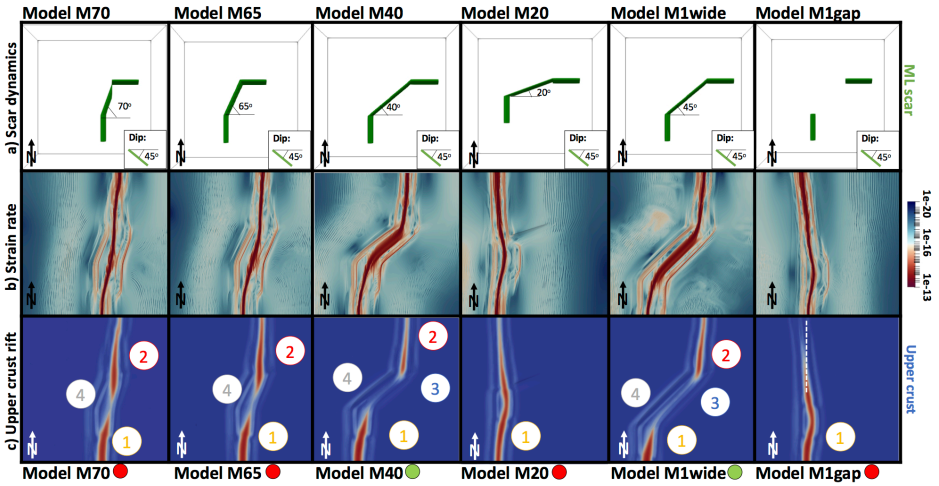

Figure 7. Rift dynamics for Model M70, M60, M40, M20, M1wide, and M1gap. (a) Initial geometry of mantle lithosphere scar (green), surface strain rate (b) alongside upper crust (blue) and spreading position (red) (c) after 15 Myr. Annotation given as (1) rifting south of modelled Davis Strait to produce new oceanic crust; (2) rifting north of Davis Strait to produce new oceanic crust; (3) segmented rift geometry; and (4) preservation of the continental crust in the Davis Strait during extension. Green circle at base of figure indicates that model passed the four-point Davis Strait checklist and red circles indicate a negative result.

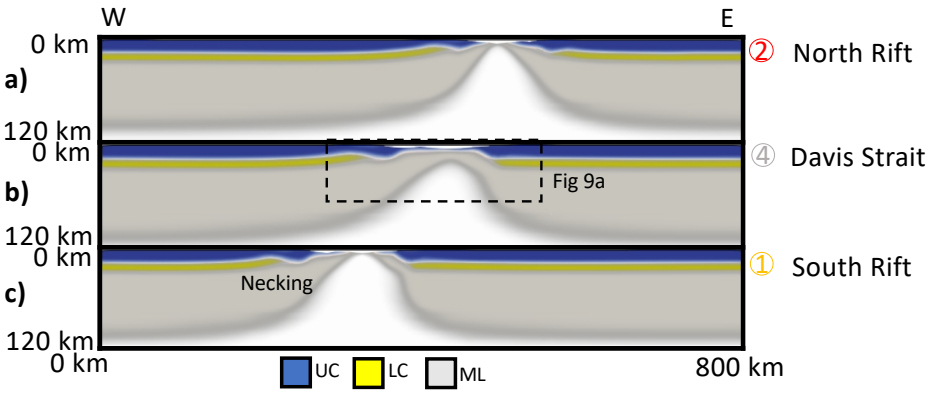

Figure 8. Lithosphere cross sections with upper and lower crust and mantle lithosphere shown across the model north rift (a), Davis Strait (b), and south rift (c) (sections as shown in Figure 6b).

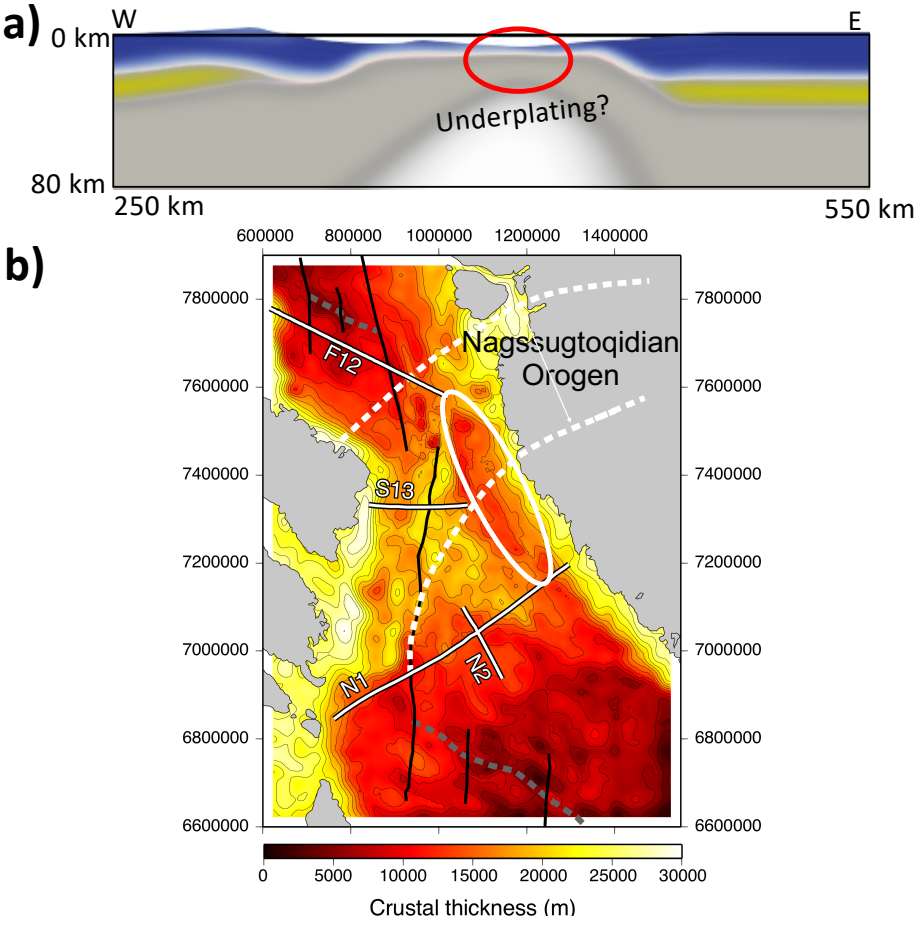

Figure 9. (a) Close-up of lithospheric cross section in Figure 8b, highlighting varying crustal thickness and shallow mantle lithosphere. (b) Gravity inversion giving the depth to Moho for the region, with coordinates relative to UTM zone 19 and ellipsoid WGS-84. White dashed lines giving the outline of the Nagssugtoqidian Orogen, with white solid circle showing an area of thinner continental lithosphere across the Davis Strait (as shown in red circle in (a)). Contour interval for the Moho map is 2000 m. Dashed grey lines represent extinct spreading centres. Black lines represent crustal faults and shear zones. White lines outlined in black refer to seismic refraction lines (N1 [*Funck et al.*, 2012], N2 [*Gerlings et al.*, 2009], F12 [*Funck et al.*, 2012], and S13 [*Suckro et al.*, 2013]), used to assess the reliability of the gravity inversion results.

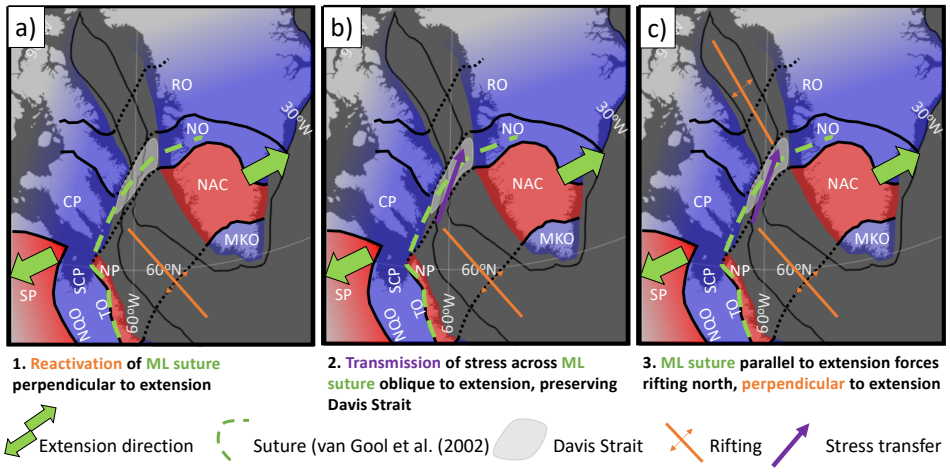

Figure 10. We propose that mantle inheritance from the Nagssugtoqidian Orogen could generate (a) south rifting, (b) creation of Davis Strait and preservation of continental lithosphere, and (c) north rifting. RO, Rinkian Orogen; NO, Nagssugtoqidian; CP, Churchill Province; NQO, New Quebec Orogen; SCP, Southern Churchill Province; TO, Torngat Orogen; NP, Nain Province; NAC, North Atlantic Craton; MKO, Makkovikian-Ketilidian Orogen.